Supporting Information

Highly efficient solar-absorber composite material based on tetrapyridylporphyrin for water evaporation and thermoelectric power generation

Yifeng Zhang*, Hanbing Yan, Xuefeng Wang, Zhenyu Zhang, Fengchun Liu, Shan Tu, Xiufang Chen

State Grid Shanxi Electric Power Research Institute, Taiyuan, Shanxi Province, 030012, P. R. China.

Experimental section

All reagents and solvents, unless otherwise specified, were obtained from J&K and Energy Chemical, and used without further purification.

Steady-state spectral measurements: The UV-vis absorption spectrum of TPyP in solvent, solid and PU+TPyP was recorded by Hitachi U-4100 ultraviolet/visible/near infrared spectrophotometer. The fluorescence spectrum and fluorescence quantum efficiency are tested on the QM8000 steady-state transient fluorescence spectrometer.

Photothermal characterizations measurements: The 730 nm and 655 nm laser beams were generated by a MDL-II laser (MDL-III-2W, 730 nm and 655 nm infrared semiconducto laser, Changchun New Industries Optoelectronics Tech. Co., Ltd, China). And the temperature response of the sample was measured with an IR thermal camera (TESTO-869).

Water evaporation performance test: Then TPyP was loaded inside PU foam by impregnating PU foam in TPyP $CHCl_3$ solution (5 mg dissolved in 0.5 mL $CHCl_3$) and dried under 50 °C, obtaining a brown color PU foam. The PU+TPyP foam was put on a quartz beaker filled with water. The sunlight, generated by a solar simulator with an optical filter for the standard AM 1.5 G spectrum (CEL-S500), irradiated at the sample under specific optical concentrations. The weight loss of water was measurement by an analytical balance and the temperature over the process was recorded by an IR thermal camera.

Thermoelectric power generation experiment: The back of the photothermal material coated with 20 mg TPyP is closely fitted with the circulating water tank to form a temperature difference and generate voltage. The open circuit voltage (Voc) of the thermoelectric is

measured and recorded with a Keithley 6514 digital multimeter/electrometer. The subsequent power generation was carried out under 1, 2 and 5 Sun respectively, and the surface temperature was collected and recorded by infrared thermal imager. The thermoelectric sheet is commercial and the model is TEC1-12706. The length is 40 mm, the width is 40 mm, and the height is 3.6 mm.

Thermal conductivity measurement: The thermal conductivity of pure PU and PU+TPyP foams were measured by a thermostat coefficient meter (C-THERM TCi).

Supplementary Note 1

The conversion efficiency was determined according to previous method. Details are as follows:

Based on the total energy balance for this system:

$$\sum_i m_i C_{pi} \frac{dT}{dt} = Q_s - Q_{loss}$$

where m_i (0.3021 g) and $C_{p,i}$ (0.8 J (g °C)$^{-1}$) are the mass and heat capacity of system components (TPyP samples and quartz glass), respectively. Q_s is the photothermal heat energy input by irradiating NIR laser to TPyP samples, and Q_{loss} is thermal energy lost to the surroundings. When the temperature is maximum, the system is in balance.

$$Q_s = Q_{loss} = hS\Delta T_{max}$$

where h is heat transfer coefficient, S is the surface area of the container, ΔT_{max} is the maximum temperature change. The photothermal conversion efficiency η is calculated from the following equation:

$$\eta = \frac{hS\Delta T_{max}}{I\left(1 - 10^{-A_{655}}\right)}$$

where I is the laser power (0.8 W cm^{-2}) and A_{655} is the absorbance of the samples at the wavelength of 655 nm.

In order to obtain the hS, a dimensionless driving force temperature, θ is introduced as follows:

$$\theta = \frac{T - T_{surr}}{T_{max} - T_{surr}}$$

where T is the temperature of TPyP, T_{max} is the maximum system temperature (135.0 °C), and T_{surr} is the initial temperature (23.0 °C).

The sample system time constant τ_s:

$$\tau_s = \frac{\sum_{i} m_i C_{p,i}}{hS}$$

thus $\dfrac{d\theta}{dt} = \dfrac{1}{\tau_s} \dfrac{Q_s}{hS\Delta T_{max}} - \dfrac{\theta}{\tau_s}$

when the laser is off, $Q_s = 0$, therefore $\dfrac{d\theta}{dt} = -\dfrac{\theta}{\tau_s}$, and $t = -\tau_s \ln \theta$

Therefore, the photothermal conversion efficiency η is 73.6%.

Supplementary Note 2

Calculation of the efficiency for solar to vapor generation. The conversion efficiency η of solar energy in photothermal assisted water evaporation was calculated as the following formula.
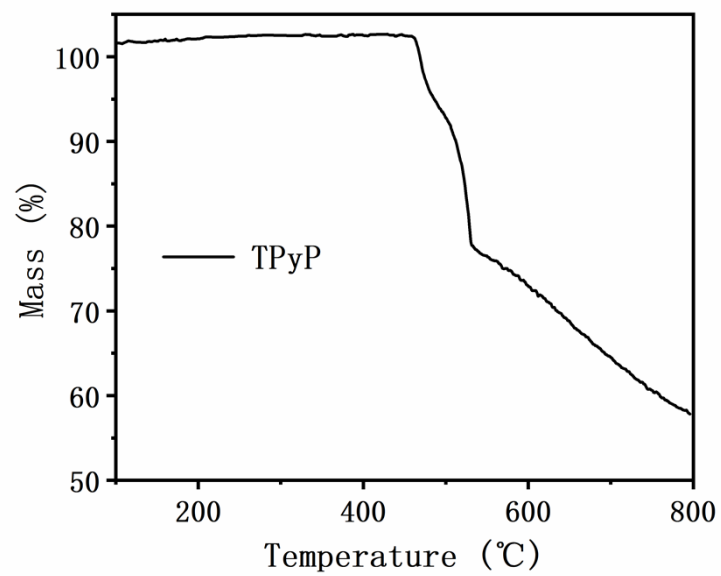
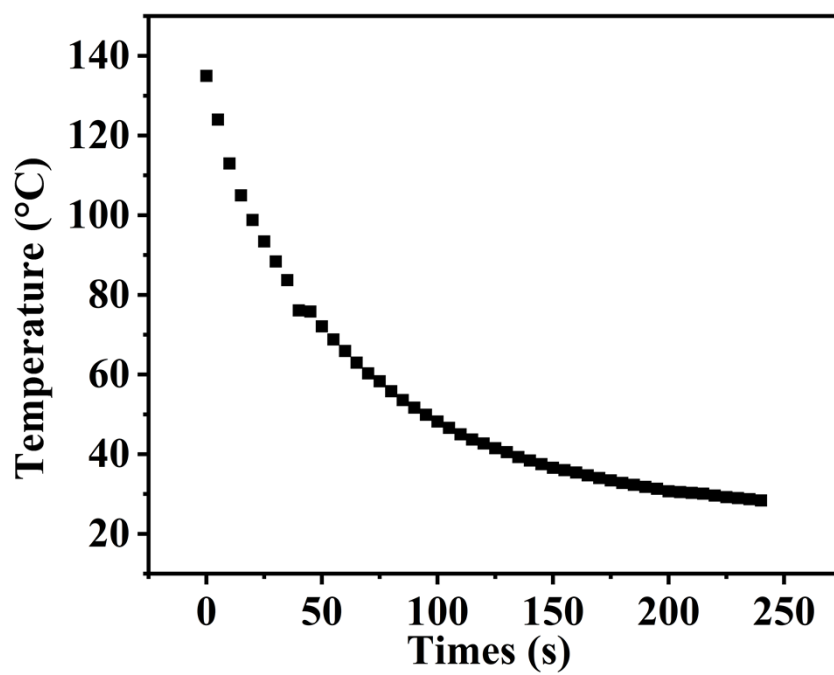$\eta = \dot{m}hLV/C_{opt}P_0$

$\dot{m} = 0.81 \ kg/m^2 \ h$

$P_0 = 1 \ kW/m^2$

$C_{opt} = 1$

As a result, evaporation efficiency $\eta = \dot{m}hLV/C_{opt}P_0 = 56\%$ when the latent heat of water vaporization at 30.4 °C is used in calculation. By the way, in this system, the solar evaporation was applied at temperatures above the environmental temperature, thus it would be unnecessary to deduct the so-called dark evaporation.

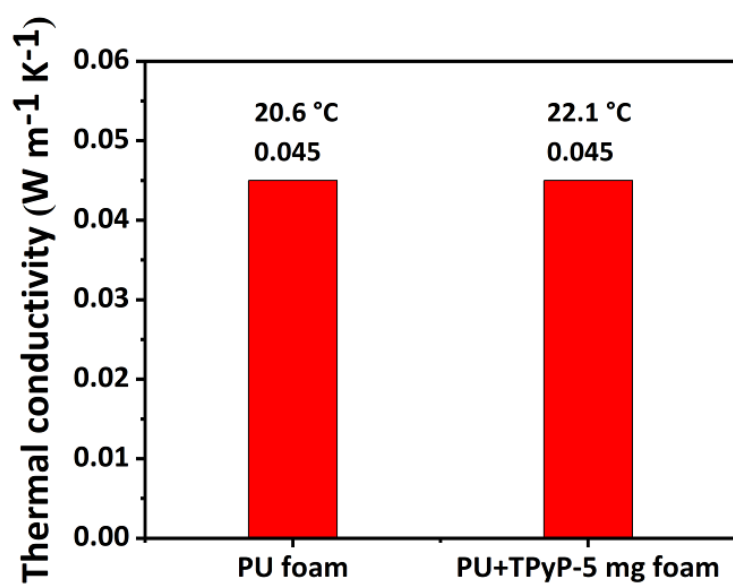**Figure S1.** TPyP thermogravimetric curve in nitrogen atmosphere.

Figure S2. The cooling curve of TPyP film after irradiation with 655 nm laser (0.8 W cm^{-2})

Equation	y = a + b*x
Slope	−92.66854 ± 1.68996
R-Square (COD	0.98461
Adj. R-Square	0.98428
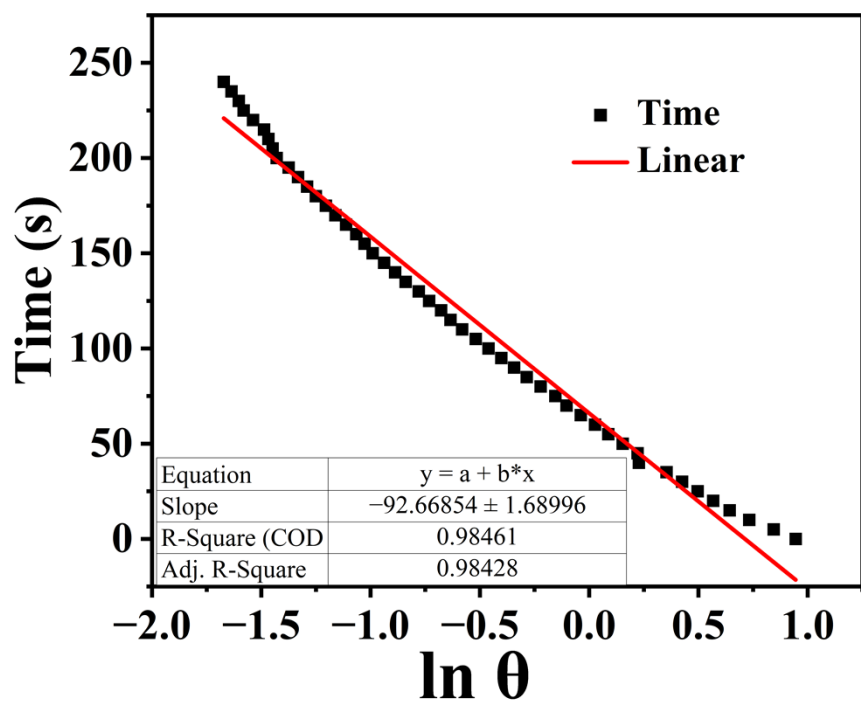
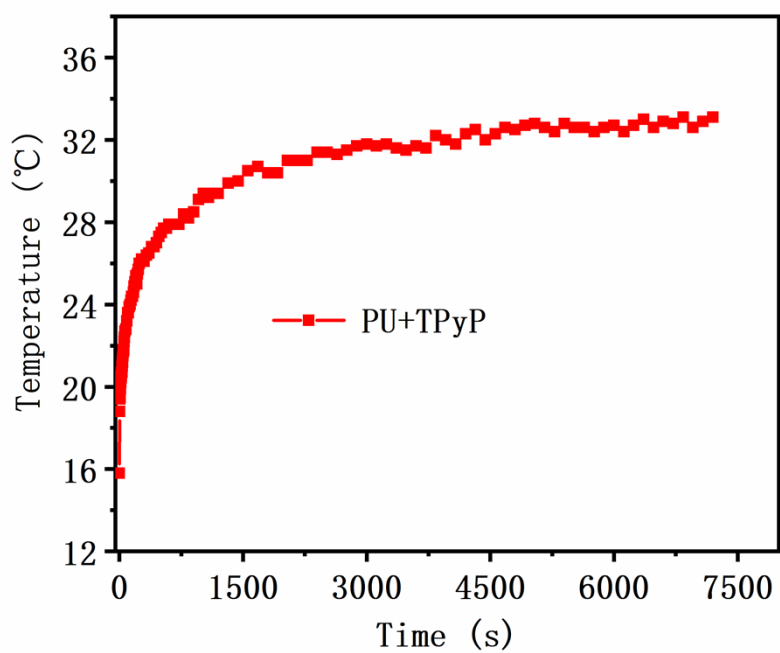**Figure S3.** The corresponding time-lnθ linear curve of TPyP film.

Figure S4. Thermal conductivities of PU and PU+TPyP foams.

Figure S5. The temperature changes of PU+TPyP foams (5 mg TPyP powder) floating on water under 1 sun for 4 h.

TableS1. The summarization of general photothermal materials for water evaporation

Material Name	Vapor evaporation rate （kg·m^{-2}·h^{-1}）	Solar-to-vapor conversion efficiency （η）	Absorption spectrum range (nm)	Ref
Carbon nanotube (CNT)	1.42	57.9%	250-2500	S1
Carbon fiber	1.47	92.5%	250-2500	S2
Hollow carbon spheres	1.45	/	/	S3
rGO–MWCNT	1.22	80.4%	300-2500	S4
CB-Al$_2$O$_3$-Cu foam	1. 31	79. 8%	280-1850	S5
Carbonized bamboo	3. 13	132.0%	250-2500	S6
GO aerogel	1.622	86.5%	200–2500	S7
Carbon sponge	1.31	85.0%	250-2500	S8
CPHSs -PVA hydrogel	1.83	82.2%	200-2000	S9
3D rGO-BFC	5.40	/	280-2500	S10
Porous Graphene	1.50	80.0%	250-2000	S11
PDA-CC	1.55	88.8%	350-1400	S12
PPY	2.12	91.5%	250-2500	S13
Organic-Small-Molecule （CR-TPE-T）	1.27	87.2%	300-1600	S14
TiO$_X$ Nanocrystals	1.32	50.3%	200–2000	S15
MXene Ti$_3$C$_2$	/	84.0%	300−1300	S16
Ni$_3$S$_2$/NF	1.29	87.2%	280–2500	S17
H$_{1.68}$ MoO$_3$	1.37	84.8%	300–2500	S18
Au/Ag PFC	1. 40	86. 3%	/	S19
Cu$_{2-X}$ S nanowires	/	89.9%	300–2500	S20
3D Cu$_x$S	1.96	94.5%	250-1100	S21

Reference:

S1.   Y. Xia, Q. Hou, H. Jubaer, Y. Li, Y. Kang, S. Yuan, H. Liu, M. W. Woo, L. Zhang and L. Gao, *Energy Environ. Sci.*, 2019, **12**, 1840-1847.

S2.   T. Li, Q. Fang, X. Xi, Y. Chen and F. Liu, *J. Mater. Chem. A*, 2019, **7**, 586-593.

S3.   J. Zhou, Z. Sun, M. Chen, J. Wang, W. Qiao, D. Long and L. Ling, *Adv. Funct. Mater.*, 2016, **26**, 5368-5375.

S4.   Y. Wang, C. Wang, X. Song, S. K. Megarajan and H. Jiang, *J. Mater. Chem. A*, 2018, **6**, 963-971.

S5.   N. Xu, J. Li, Y. Wang, C. Fang, X. Li, Y. Wang, L. Zhou, B. Zhu, Z. Wu and S. Zhu, *Sci. Adv.*, 2019, **5**, eaaw7013.

S6.   Y. Bian, Q. Du, K. Tang, Y. Shen, L. Hao, D. Zhou, X. Wang, Z. Xu, H. Zhang and L. Zhao, *Adv. Mater. Technol.*, 2019, **4**, 1800593.

S7.   X. Hu, W. Xu, L. Zhou, Y. Tan, Y. Wang, S. Zhu and J. Zhu, *Adv. Mater.*, 2017, **29**, 1604031.

S8.   L. Zhu, M. Gao, C. K. N. Peh, X. Wang and G. W. Ho, *Adv. Energy Mater.*, 2018, **8**, 1702149.

S9.   M. Tan, J. Wang, W. Song, J. Fang and X. Zhang, *J. Mater. Chem. A*, 2019, **7**, 1244-1251.

S10.   Y. Wang, X. Wu, P. Wu, J. Zhao, X. Yang, G. Owens and H. Xu, *Sci. Bull.*, 2021, **66**, 2479-2488.

S11.   Y. Ito, Y. Tanabe, J. Han, T. Fujita, K. Tanigaki and M. Chen, *Adv. Mater.*, 2015, **27**, 4302-4307.

S12.   X. Wu, L. Wu, J. Tan, G. Y. Chen, G. Owens and H. Xu, *J. Mater. Chem. A*, 2018, **6**, 12267-12274.

S13.   W. Li, Z. Li, K. Bertelsmann and D. E. Fan, *Adv. Mater.*, 2019, **31**, 1900720.

S14.   G. Chen, J. Sun, Q. Peng, Q. Sun, G. Wang, Y. Cai, X. Gu, Z. Shuai and B. Z. Tang, *Adv. Mater.*, 2020, **32**, 1908537.

S15.   M. Ye, J. Jia, Z. Wu, C. Qian, R. Chen, P. G. O'Brien, W. Sun, Y. Dong and G. A. Ozin, *Adv. Energy Mater.*, 2017, **7**, 1601811.

S16.   R. Li, L. Zhang, L. Shi and P. Wang, *ACS Nano*, 2017, **11**, 3752-3759.

S17.   H. Jiang, L. Ai, M. Chen and J. Jiang, *ACS Sustainable Chem. Eng.*, 2020, **8**, 10833-10841.

S18.   Q. Zhu, K. Ye, W. Zhu, W. Xu, C. Zou, L. Song, E. Sharman, L. Wang, S. Jin and G. Zhang, *The Journal of Physical Chemistry Letters*, 2020, **11**, 2502-2509.

S19.   H. D. Kiriarachchi, F. S. Awad, A. A. Hassan, J. A. Bobb, A. Lin and M. S. El-Shall, *Nanoscale*, 2018, **10**, 18531-18539.

S20.   N. Li, D. Yin, L. Xu, H. Zhao, Z. Liu and Y. Du, *Materials chemistry frontiers*, 2019, **3**, 394-398.

S21.   W. Huang, P. Su, Y. Cao, C. Li, D. Chen, X. Tian, Y. Su, B. Qiao, J. Tu and X. Wang, *Nano Energy*, 2020, **69**, 104465.